Experiment and simulation of layered bioretention system for hydrological performance

Chunbo Jiang, Jiake Li, Huaien Li and Yajiao Li

ABSTRACT

Bioretention can reduce surface runoff, slow down peak flow, and delay peak time by increasing the infiltration capacity of the underlying surface. The media structure directly affects the performance of bioretention systems. Four pilot tanks with different media configuration were built, and hydraulics and water volume reduction were studied though intermittent, simulated storm events. The results showed that water volume and peak flow reduction rate were the most stable and efficient for #1 (fly ash mixing sand, 1:1 by volume) than other systems, which were 58.6–67.9% and 72.0–86.4%, respectively. Partial least squares regression (PLS) was used to build a model for the relation between water volume reduction rate and its influencing factors ($R^2 = 0.76$), and the factors that influence bioretention water volume reduction were ranked from strongest to weakest as follows: infiltration rate (IR) > submerged area height (SAH) > inflow volume (IV) > antecedent dry time (ADT). In addition, volume reduction rate exhibited a positive correlation with ADT and SAH, and a negative correlation with IR and IV. Three water transfer simulations with different infiltration rates were conducted using HYDRUS-1D under designed inflow conditions, and the minimum relative error is obtained for #1.

Key words | bioretention, HYDRUS-1D, media structure, partial least squares

Chunbo Jiang
Jiake Li (corresponding author)
Huaien Li
State Key Laboratory of Eco-hydraulics in Northwest Arid Region of China,
Xi'an University of Technology,
Xi'an 710048,
China
E-mail: *xaut_ljk@163.com*

Yajiao Li
School of Architecture and Civil Engineering,
Xi'an University of Science and Technology,
Xi'an 710054,
China

INTRODUCTION

Rapid urbanization worldwide is a major contributor to changes in runoff quantity, such as increase in runoff volume and rates, reduction in runoff lag time and groundwater recharge, and has caused a series of social environmental problems (Demuzere *et al.* 2014; Liu *et al.* 2017). In China, inadequate drainage capacities and older, aging drainage facilities are the prominent issues for storm water management. Due to the increase of impervious areas, pumping station operation for urban drainage systems has increased, increasing energy consumption and treatment costs accordingly (Nie 2008). Urban rainwater utilization is an effective method to alleviate urban water crisis and improve the urban water environment, and it has drawn widespread attention worldwide.

Green infrastructure (GI) is used to deal with urban runoff at the source, such as green roofs, rain gardens, bioretentions, etc. Compared to the traditional rapid discharge method, GI technologies maintain runoff volume, peak flow, and time to flood peak in developed areas consistently compared with the original condition, using infiltration, retention, storage, and other stormwater treatment measures (Versini *et al.* 2018). Several studies have demonstrated that the impacts of development on hydrologic regimes in urban areas could be reduced via bioretention (Davis *et al.* 2012; Page *et al.* 2012). Gülbaz & Kazezyılmaz-Alhan (2016) found that different soil characteristics have considerable effects on the hydrological performance of bioretention due to different infiltration capacities of various combinations

doi: 10.2166/wrd.2019.008

of vegetative soil, sand, and turf, and high sand ratio, which results in a decrease in time lag between the peak inflow and outflow and an increase in the peak outflow. More simulations were conducted to evaluate hydrological performance of bioretention systems. Hydrologic models such as SWMM and DRAINMOD performed well in simulating the long-term effects of bioretention facilities (Brown *et al.* 2013; Cipolla *et al.* 2016). The HYDRUS model has been used in agricultural and environmental fields, and the migration of water and solutes can be simulated comprehensively with this model, which requires minimal input data and whose results are reliable (Ramos *et al.* 2011; Yi & Fan 2016). The HYDRUS-1D model was applied to simulate the runoff generation processes for bioretention facilities with different designed precipitation frequency and filter media (Yin *et al.* 2015). The simulated results indicate that: as recurrence interval changed from $P = 100\%$ to $P = 1\%$, rainfall depth from 48.1 mm (1.9 in.) to 423.4 mm (16.7 in.) in 24 hours, the percentage of infiltration volume as total inflow volume changed from 90.7% to 25.8% for bioretention.

The types and combinations of media play critical roles in bioretention hydrologic performance. A pilot-scale bioretention experiment and theoretical analysis are carried out to: (i) identify hydrologic performances of bioretention tanks under different infiltration rate (IR), submerged area height (SAH), inflow volume (IV), and antecedent dry time (ADT); (ii) explore the effects of water volume regulation for bioretention tanks under dry and wet conditions; (iii) establish a correlation model between water volume reduction rate and its influencing factors; and (iv) simulate rainfall migration in bioretention under specified conditions using HYDRUS-1D.

MATERIALS AND METHODS

Experiment devices

Four bioretention facilities (Figure 1) were designed and constructed in the outdoor test field of Xi'an University of Technology. The specifications of each tank are as follows: 2 m × 0.5 m × 1.05 m (length × width × depth). Each tank contains the following layers from top to bottom: ponding depth (15 cm), covering layer (5 cm), planting soil layer (30 cm), special packing layer (40 cm), and gravel drainage layer (15 cm) except #4 (with planting soil (PS) as media, and without special packing layer). Moreover, a perforated drain pipe was set at the bottom of the gravel drainage layer and wrapped with permeable geotextile. A permeable geotextile was also set between each layer.

Infiltration process in the layered bioretention facility is divided into three forms, which are, a high permeability layer over a lower permeability layer (#1), a low permeability layer over a higher permeability layer (#3), and homogeneous infiltration media (#4). The special packing layers of these tanks are as follows: planting soil (#1),

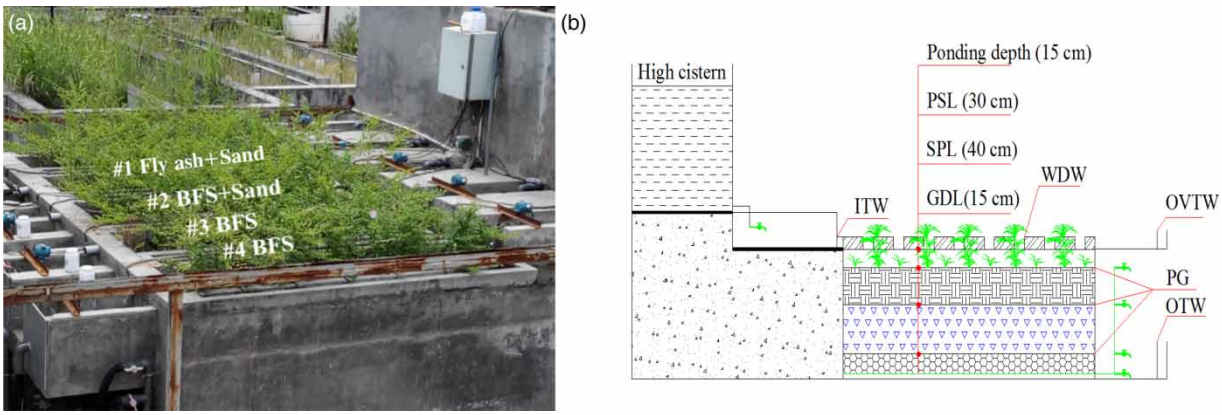

Figure 1 | Experimental device. Construction of the test tank included ponding depth, mulch, planting soil layer (PSL), special packing layer (SPL), gravel drainage layer (GDL) from top to bottom, BFS for blast furnace slag, WDW for water distribution weir, and ITW, OTW, and OVTW for inflow, outflow, and overflow triangle weir, respectively, and PG for permeable geotextile.

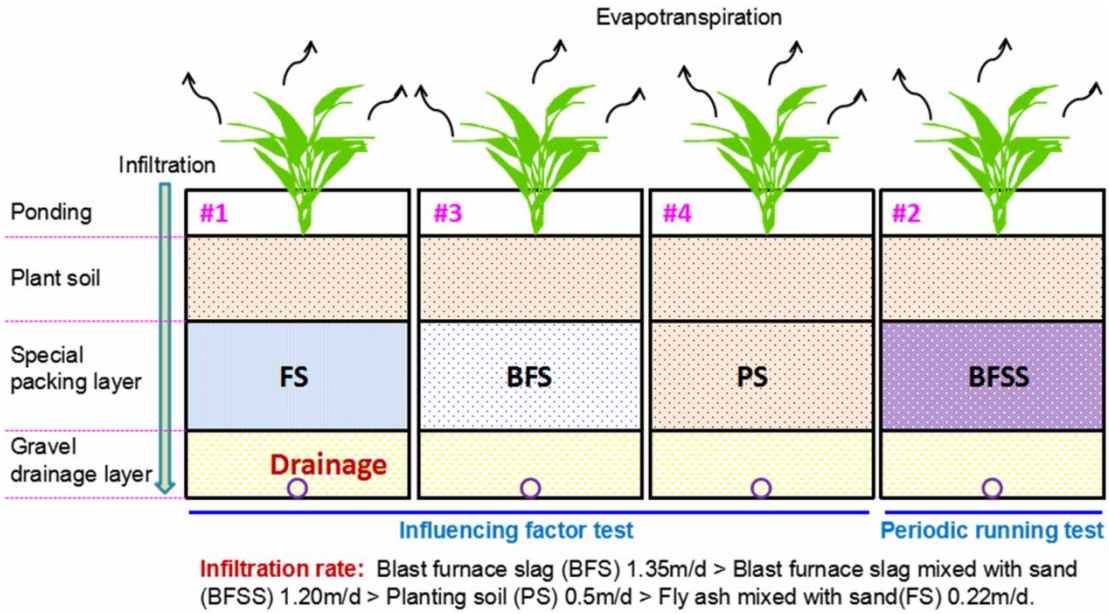

Figure 2 | Vertical structure of the experimental device.

blast furnace slag (#3), and fly ash mixed with sand (volume ratio, 1:1, #4), which were selected for the influencing factor effect test to identify the relationship between water volume reduction rate and ADT, SZH, IV, and IR. Tank #2 was selected for the period running effect test without considering the impact of ADT and SZH, and the special packing layer of this tank is blast furnace slag mixed with sand (BFSS) (volume ratio, 1:1). Infiltration rates of blast furnace slag (BFS), BFSS, PS and fly ash mixed with sand (FS) are 1.35 m/d, 1.20 m/d, 0.5 m/d, and 0.22 m/d, respectively (Figure 2). Particle sizes were: BFS (0.6–1.5 cm), FS (<0.1 cm), sand (<0.3 cm), and gravel (1.5–3 cm). The results of soil particles analysis indicated that the percentage of clay, silt, and sand of plant soil in this test were 3.5%, 90.4%, and 6.1%, respectively.

Monitoring and analysis methodology

Nine tests were conducted for tanks #1, #3, and #4 to study the running effect of bioretention under different inflow hydraulic loading, SZH, ADT, and IR (Table 1). The rainfall duration of 120 min and return periods of two years and five years were used in the Xi'an rainstorm intensity–duration–frequency formula (Lu *et al.* 2010). Two designed inflow volumes (573.85 L and 427.16 L) were determined, which respectively corresponded to the rainfall of 1.3 in. and 1.0 in. for the actual catchment area (17 m^2). For #2, a quantity test was conducted alternatively under five-year and two-year design rainfall intensities, and the ADT between every two rain events was 15 days to explore the effects of water volume regulation for bioretention ponds under dry and wet conditions. A complete rainfall-runoff process, including ascent–peak–recession, must be simulated in this study. The effect was better observed when the peak flow or storage volume was calculated with the Chicago pattern

Table 1 | Scheme of the influencing factor test for #1, #3, and #4

Test number	Test date	SZH (mm)	ADT (day)	Recurrence interval (yr)	Inflow volume (L)
Test 1	5/20/2015	0	7	5	573.85
Test 2	5/27/2015	150	7	5	573.85
Test 3	6/30/2015	0	7	5	573.85
Test 4	6/18/2015	0	15	5	573.85
Test 5	6/25/2015	0	7	5	573.85
Test 6	6/28/2015	0	3	5	573.85
Test 7	7/05/2015	0	7	2	427.16
Test 8	7/12/2015	0	7	5	573.85
Test 9	7/19/2015	0	7	5	573.85

(also known as Keifer and Chu rain pattern) (Cen *et al.* 1998). The Chicago rainfall pattern was developed by considering a rainstorm intensity formula traditionally used to determine the peak flow of short-duration precipitation (less than 3 h), and the rainfall peak coefficient was set to 0.3 in these tests.

Triangle weirs with 30° angles were set at the inflow, outflow, and overflow points of the system. These weirs were installed with level monitoring gauges. Inflow and outflow were calculated by Equation (1), inflow and outflow volume were calculated by Equation (2), and water volume reduction rate and peak flow reduction rate calculated as shown by Equations (3) and (4):

$$Q = \frac{8}{15}\mu tg\frac{\theta}{2}\sqrt{2g}h^{\frac{5}{2}} \quad (1)$$

where Q is the water flow, m^3/s; h is the geometric head of the weir, m; θ is the weir crest angle; μ is the discharge coefficient, 0.6; and g is the acceleration of gravity, 9.808 m/s^2.

$$V_{inflow/outflow} = \sum Q_{(t)}\Delta t \quad (2)$$

$$R_v = \frac{V_{inflow} - V_{outflow}}{V_{inflow}} \times 100\% \quad (3)$$

$$R_p = \frac{Q_{\max(inflow)} - Q_{\max(outflow)}}{Q_{\max(inflow)}} \times 100\% \quad (4)$$

where R_v is the water volume reduction rate; R_p is the peak flow reduction rate; Q_t is the flow during the interval time; $V_{inflow/outflow}$ is the volume of inflow or outflow; $Q_{max(inflow/outflow)}$ is the inflow/outflow peak flow.

RESULTS AND DISCUSSION

Analysis of the influencing factors test

Tanks #1 (fly ash mixed with sand), #3 (blast furnace slag), and #4 (PS) were used as the research objects, and the results of eight tests are presented in Table 2. Overall, the water quantity reduction effect of bioretention was considerable under a return period of five years in a 120 min rainfall event, and water volume reduction rate reached 50% approximately. Water quantity reduction rates for #1 were fairly stable in the eight tests (58.59% to 67.93%). Water quantity reduction rates (27.35% to 55.78% or 25.83% to 61.57%) for #3 and #4 were unsteady in each test and were significantly affected by the influencing factors (IV, ADT, SZH, and IR).

The filtration coefficient is an important design parameter that depends on media characteristics and structure. Three layers (PS layer, special packing layer, and gravel drainage layer) have a series connected structure, and permeability was determined by the layer with the least saturated soil permeability. Water ponding occurred

Table 2 | Experiment results of internal and external influencing factors

	#1			#3			#4		
	R_v/%	R_p/%	T/min	R_v/%	R_p/%	T/min	R_v/%	R_p/%	T/min
Test 1	–	–	–	–	–	–	–	–	–
Test 2	61.12	80.60	28	54.62	58.37	24	56.60	61.96	23
Test 3	58.59	79.29	21	48.68	58.97	11	51.35	40.79	9
Test 4	65.94	84.72	30	40.05	51.90	10	51.11	67.65	8
Test 5	65.29	85.21	17	40.74	21.19	9	45.83	45.29	10
Test 6	58.82	71.99	19	40.01	27.35	8	46.76	50.80	5
Test 7	66.24	78.10	26	46.11	76.48	15	61.57	66.00	9
Test 8	60.99	80.87	31	45.78	68.93	12	53.55	61.24	7
Test 9	61.93	86.44	26	40.15	24.05	13	50.97	62.37	7

Note: Test 1 is the pre-test.

in #1, and this tank also exhibited the best performance in terms of water quantity reduction. Thus, the best water retention effect was observed in the bioretention system in which saturated infiltration occurred. In this study, the form of rain-type in the Chicago pattern was used as the inflow, and the media of the bioretention system was also arranged in different layered structures. The results exhibited obvious differences in the retention time of different tanks for stormwater runoff. The retention time of tank #1 ranged from 17 min to 31 min, and most of them are concentrated in 25 min. Minimal difference occurred between the retention time of tanks #3 and #4. Further, the retention time was 8 min to 24 min and 5 min to 23 min, respectively, and centered at around 10 min. During the eight rain events, peak discharge was effectively reduced by these facilities. Similar to the water quantity reduction effect, the peak discharge rate of tank #1 was relatively stable, and variation ranged from 72.0% to 86.4%. The peak discharge rates of the tanks with blast furnace slag or PS as special packing were more variable and presented as follows: 21.2% to 76.5% and 40.8% to 66.0%.

Analysis of period running effect test

The period running test began in May 2015 and ended in December 2015. For those eight months, simulated rainfall tests were conducted every 15 d at #2 (special layer is BFSS). In order to study the water quantity regulation effect of #2 bioretention tank under two design recurrence periods and wet–dry alternation conditions, the 15 tests under design rainfall intensity of five years (a total of eight tests) and two years (a total of seven tests) recurrence interval were conducted, respectively (Figure 3). #2 water volume reduction rates were more than 55.8% and 60.0%, respectively, under five-year and two-year return periods. The range difference was 23.3% and 20.9%, respectively, and the effect of water reduction was not greatly affected by seasonal changes, and it still had a good effect in winter.

Different hydrological conditions affect the plant transpiration, evapotranspiration, and soil restoration, thus affecting the water regulation effect of the bioretention system. Hatt *et al.* (2009) hold that biofilters were shown to effectively attenuate peak runoff flow rates by at least 80%, and water retention was found to be most influenced by inflow volumes in light to medium storms, which reduced runoff volumes by 33% on average. The results of 15 events indicated that peak flow reduction rate ranged from 55.1% to 81.3%, and lag time ranged from 14 min to 24 min under five-year design rainfall intensities in this study. Meanwhile, peak flow reduction rate ranged from 57.9% to 88.2% and the retention time ranged from 15 min to 26 min under two-year design rainfall intensities. After October, the peak flow reduction rates of the test tanks were significantly higher. However, retention time did not exhibit a particular pattern because of the strong influence of other factors which were inflow volume, rainfall pattern, media structure, and so on.

Considering seasonal temperature variations, the water volume reduction effect of bioretention was affected by various factors. On the one hand, the reduction effect was related to soil texture. The silt fraction of the test soil was higher than other fractions, and its retention capacity was poor. On the other hand, the reduction effect was related to ET. The plants growing in the facilities did well with plenty of sunlight. In summer, ET is high and surface

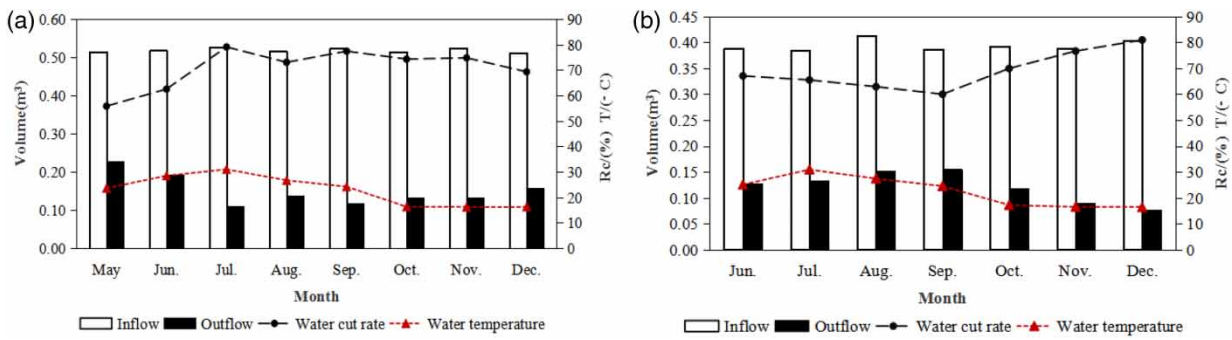

Figure 3 | Water process under different return periods: (a) five years and (b) two years.

soil moisture is low. In winter, plant growth is slow due to the plants entering a dormant phase. Soil water evaporation was minimized by the surface withered grass and fallen leaves. Evidently, soil moisture content was also affected by the water volume reduction effect. In addition, soil permeability decreased significantly when ground crust appeared, whereas bioretention outflow increased because of uneven infiltration and preferential flow.

Modeling analysis of the water volume reduction effect

This study determined the relationship among water volume reduction, IV, ADT, SZH, and IR through SIMCA-P software. Only one dependent variable Y (water volume reduction rate) was used in the results of #1, #3, and #4. Independent variable X includes IV, ADT, SZH, and IR. ADT and IR comprised three levels, whereas IV and ADT factors consisted of two levels. Curve analysis showed that the relationship between water volume reduction rate and ADT or packing factor was highly linear. A standardization equation, i.e., Equation (5), and the equation of primitive variables, i.e., Equation (6), were obtained using the partial least squares (PLS) method:

$$y_0 = a_1x_1 + a_2x_2 + a_3x_3 + a_4x_4 \quad (5)$$

$$y_1 = b_0 + b_1x_1 + b_2x_2 + b_3x_3 + b_4x_4 \quad (6)$$

where y_0 and y_1 are the water volume reduction rates, %; x_1 is the inflow hydraulic load, L; x_2 is the ADT, d; x_3 is the SZH, mm; and x_4 is the packing infiltration rate, m/d; $a_1 \sim a_4$, and $b_0 \sim b_4$ are variable coefficients.

Model samples are provided in Table 3. Tests 3 and 8 (ADT was 7 days without SZH) were selected for model validation (Table 4). The standardized variable regression equation was as Equation (7), and the original variable regression equation as Equation (8):

$$y^* = -0.276x_1 + 0.106x_2 + 0.286x_3 - 0.789x_4 \quad (7)$$

$$\hat{y} = 79.9853 - 0.041x_1 + 0.280x_2 + 0.048x_3 - 14.494x_4 \quad (8)$$

The difference between the value of simulation using PLS and the experimental value was insignificant. The coefficient of determination R^2 was 0.76, and residuals were within ±10%. The relative importance expressed by the standardized regression coefficient was related to the dispersion degree among dependent variables in a particular case. The standardized regression coefficient was related to undulation degree of the independent variable. If the undulation degree is large, then the relative importance will be high. The standardized regression coefficient was positively relevant to the standard deviation of the independent

Table 3 | Model samples of the water cut rate and the influencing factors

Test number	Tank number	IV (L)	ADT (d)	SZH (mm)	IR (m/d)	WCR (%)
Test 1	#1	529.73	7	0	0.22	57.25
	#3	532.14	7	0	1.35	46.25
	#4	520.69	7	0	0.5	49.15
Test 2	#1	536.49	7	150	0.22	61.12
	#3	535.11	7	150	1.35	54.62
	#4	532.53	7	150	0.5	56.60
Test 4	#1	525.88	15	0	0.22	65.94
	#3	539.16	15	0	1.35	40.05
	#4	525.43	15	0	0.5	51.11
Test 5	#1	532.82	7	0	0.22	65.29
	#3	525.21	7	0	1.35	40.74
	#4	515.11	7	0	0.5	45.83
Test 6	#1	546.71	3	0	0.22	58.82
	#3	533.03	3	0	1.35	40.01
	#4	524.76	3	0	0.5	46.76
Test 7	#1	353.76	7	0	0.22	66.24
	#3	361.49	7	0	1.35	46.11
	#4	359.63	7	0	0.5	61.57
Test 9	#1	518.86	7	0	0.22	61.93
	#3	517.71	7	0	1.35	40.15
	#4	503.54	7	0	0.5	50.97

Note: IV is inflow volume; ADT is antecedent dry time; SZH is submerged zone height; IR is media infiltration rate; WCR is water cut rate.

Table 4 | Test samples of the measured and predicted water cut rates and the influencing factors

Test number	Tank number	IV (L)	ADT (d)	SZH (mm)	IR (m/d)	WMV (%)	WPV (%)
Test 3	#1	526.03	7	0	0.22	58.59	57.19
	#3	531.52	7	0	1.35	48.68	40.59
	#4	520.81	7	0	0.5	51.35	53.35
Test 8	#1	507.05	7	0	0.22	60.99	57.97
	#3	525.44	7	0	1.35	45.78	40.84
	#4	534.41	7	0	0.5	53.55	52.79

Note: WMV is measured and predicted water cut rates; WPV is predicted water cut rates.

variable. The increase of the independent variable dispersion degree resulted in the increase of the relative importance in this particular case. Due to the packing IR increase, water exfiltration rate will be increased in the bioretention system. Winston *et al.* (2016) monitored three bioretention cells constructed in low permeability soils in northeast Ohio. They found that the exfiltration rate and the internal water storage (IWS) zone thickness were the primary determinants of volume reduction performance. Similarly, the PLS analysis results in this study showed that special packing IR was the most important influencing factor for the water volume reduction rate of bioretention. Other influencing factors, in order of importance, were as follows: SZH > IV > ADT (Figure 4(a)).

Treatment performance of bioretention tanks closely depends on hydrologic and hydraulic factors such as rainfall characteristics and inflow and outflow discharges. With the reduction of infiltration capacity, the bioretention system can achieve the effect of slow release and slow drainage for rainwater runoff, giving full play to the water holding and retention capacity of the media. When infiltration technology is used to treat rainwater for harvest, the permeability coefficient is not less than 10^{-5} m/s, when infiltration technology is used to treat rainwater to recharge groundwater, the permeability coefficient is generally not less than 10^{-6} m/s (Che & Li 2006). As permeability coefficient increases, the system can resist heavy rainfall events, controlling ponding and overflow events occurring. However, the downward migration of fine particles is more likely to cause system blockage in a high IR bioretention system. Mangangka *et al.* (2015) confirmed that the ADT plays an important role in influencing treatment performance. ADT determines the initial moisture content of bioretention media, and 15, 7, and 3 days in tests 4, 5, and 6 were compared for volume reduction in this study. The establishment of SZH creates the denitrification condition for the pollutant removal. Meanwhile, considering the duration and the frequency of ADT, the study found that the minimum SZH has a depth of 300 mm (11.8 in.), which can withstand 5 consecutive weeks of drought (Payne *et al.* 2014). The correlation analysis between reduction rate and influencing factors indicated that water volume reduction rate and ADT or SZH were positively correlated. Moreover, water volume reduction rate and IV or IR were negatively correlated (Figure 4(b)).

Simulation of water volume retention based on HYDRUS-1D model

Water movement equation

HYDRUS-1D is a model published by the International Groundwater Modeling Center (IGWMC) for simulating saturated (saturated–unsaturated) water movement, solute transport, heat transfer, and crop growth in porous media. A 1D vertical soil moisture movement basic equation, which disregards the horizontal and sideways movements of soil moisture, is presented as follows:

$$\frac{\partial \theta}{\partial t} = C(h)\frac{\partial h}{\partial t} = \frac{\partial}{\partial z}\left[K(\theta)\left(\frac{\partial h}{\partial z} - 1\right)\right] - S(h) \quad (9)$$

where θ is the soil moisture content; $C(h)$ is the water capacity; h is the pressure head, cm; t is the time, s; k is

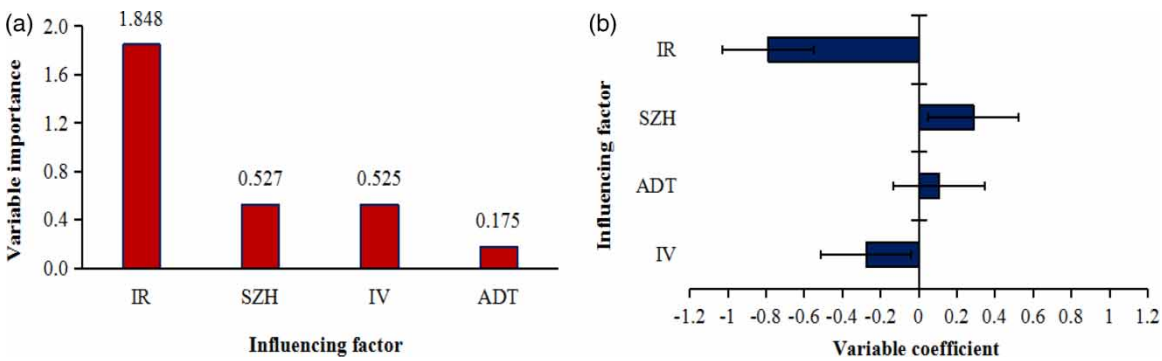

Figure 4 | Analysis of modeling results: (a) importance analysis of influencing factors and (b) correlation analysis.

the soil hydraulic conductivity, $L \cdot T^{-1}$; *S(h)* is the root water uptake per unit time and per unit volume; and z is the vertical coordinate, cm, which regards the downward direction as positive.

The soil moisture characteristic curve was described using a Van Genuchten equation as follows:

$$\frac{\theta - \theta_r}{\theta_s - \theta_r} = \left[\frac{1}{1 + (\alpha h)^n}\right]^m \tag{10}$$

$$K = K_s S_e^{\lambda}\left[1 - \left(1 - S_e^{\frac{n}{n-1}}\right)^{\frac{n-1}{n}}\right]^2 \tag{11}$$

$$S_e = (\theta - \theta_r)/(\theta_s - \theta_r) \tag{12}$$

where θ is the volume moisture content, cm^3/cm^3; θ_r is the residual retention water content; θ_s is the moisture content at saturation; h is the soil suction, cm; K_s is the saturated hydraulic conductivity, $L \cdot T^{-1}$; S_e is the effective saturation, -; and λ, m, n, and α are fitting parameters, where $m = 1 - 1/n$.

The underlying soil properties are significant to bioretention cell hydrological performance. Disturbances of Van Genuchten model parameters θ_r, θ_s, α, n affect the shape of the soil water characteristic curve significantly. Although the disturbance of K_s does not affect the shape of soil water characteristic curve, K_s determines the soil water conductivity. The study found that K_s and θ_s are the key factors affecting the bottom flux (Wang *et al.* 2013). Baek *et al.* (2017) also found that K_s and constant n from the Van Genuchten equation can significantly affect the bioretention mechanism.

Initial conditions and boundary conditions of moisture movement

The simulation initial conditions setting indicated that soil profile water content was equally distributed at the beginning of the study, such that $\theta(0,x) = \theta_i$ and θ_i was the initial soil moisture. Soil boundary conditions were divided into three types: concentration, flux, and mixed types. For the first type, the water content of soil water supply boundary was constant. For the second type, which was suitable for the rainfall–infiltration process, soil surface water supply intensity remained unchanged and overland runoff did not appear. For the third type, which was a combination of the first and second types, all the rainwater infiltrated during the precipitation process. Moreover, soil moisture was under saturation condition with ponding at the soil surface (concentration type) when rainfall intensity was greater than infiltration intensity.

$$\text{The first type}: \theta(t, 0) = \theta_1 \text{ or } \phi(t, 0) = \phi_1, \tag{13}$$

$$\text{The second type}: -D(\theta)\frac{\partial \theta}{\partial z} + K(\theta) = R(t) t > 0, z = 0 \tag{14}$$

where $D(\theta)$ is the diffusion rate, θ is the boundary soil moisture content, ϕ_1 is the boundary soil water potential, and $R(t)$ is the rainfall intensity. The bottom boundary condition was set as free drainage.

Parameter calibration and model validation of moisture movement

When HYDRUS was used for model calculation, bioretention tanks were simplified: (i) the packing of each layer was uniform and isotropic; (ii) soil structure and porosity condition were unlikely to change during the infiltration process; (iii) only a single phase flow (soil moisture movement) existed regardless of vapor movement; (iv) soil air did not affect soil moisture movement; (v) only a monotonic process (single wet or moisture removal process) was considered regardless of the hysteresis effect; (vi) the effects of plant roots and temperature were ignored. Tanks #1, #3, and #4 were used as the objects in this study. The model was calibrated based on the test data under two-year design rainfall intensity and was verified based on the test data under five-year design rainfall intensity. The initial time was 0 min, and the simulation period was 120 min. The iterative calculation parameters were set at default values, and van Genuchten–Mualem model was chosen as the soil moisture characteristic curve. The initial soil moisture of the upper, middle, and lower layers was 15%, 19%, and 20%, respectively. The soil hydraulic characteristic parameters of bioretention were adjusted based on the measured value and the characteristic parameters after calibration and validation

Table 5 | Bioretention soil hydraulic characteristic parameters

Bioretention media	θ_r	θ_s	Alpha [1/cm]	n	K_s [cm/min]	l
Upper	0.072	0.422	0.025	1.690	0.095	0.5
#1 middle	0.065	0.410	0.075	1.890	0.079	0.5
#3 middle	0.055	0.431	0.021	1.540	0.135	0.5
#4 middle	0.072	0.422	0.025	1.690	0.095	0.5
Lower	0.080	0.459	0.013	1.449	0.751	0.5

(Table 5). A comparison of the predicted and measured values is shown in Figure 5.

Sun & Wei (2011) simulated the hydrological effects of bioretention tanks in terms of runoff reduction, groundwater infiltration, ponding time, and total treated volume. The results showed that discharge ratio was the most important influencing factor to runoff reduction, groundwater recharge, and water ponding time. In addition, studies showed that water retention depends strongly on the quantity of rainfall per storm event (Lee *et al.* 2013). Inflow volume is decided by rainfall intensity, rainfall duration, and discharge ratio. The differences between the simulation values using HYDRUS-1D and the measured values were insignificant for the infiltration process during a 120 minutes event. #1 was relatively optimal, and the average relative errors under two year and five year design rainfall intensity were 20.0% and 25.7%, respectively. The differences between the predicted values were close to the measured values for #1, #3, and #4 systems.

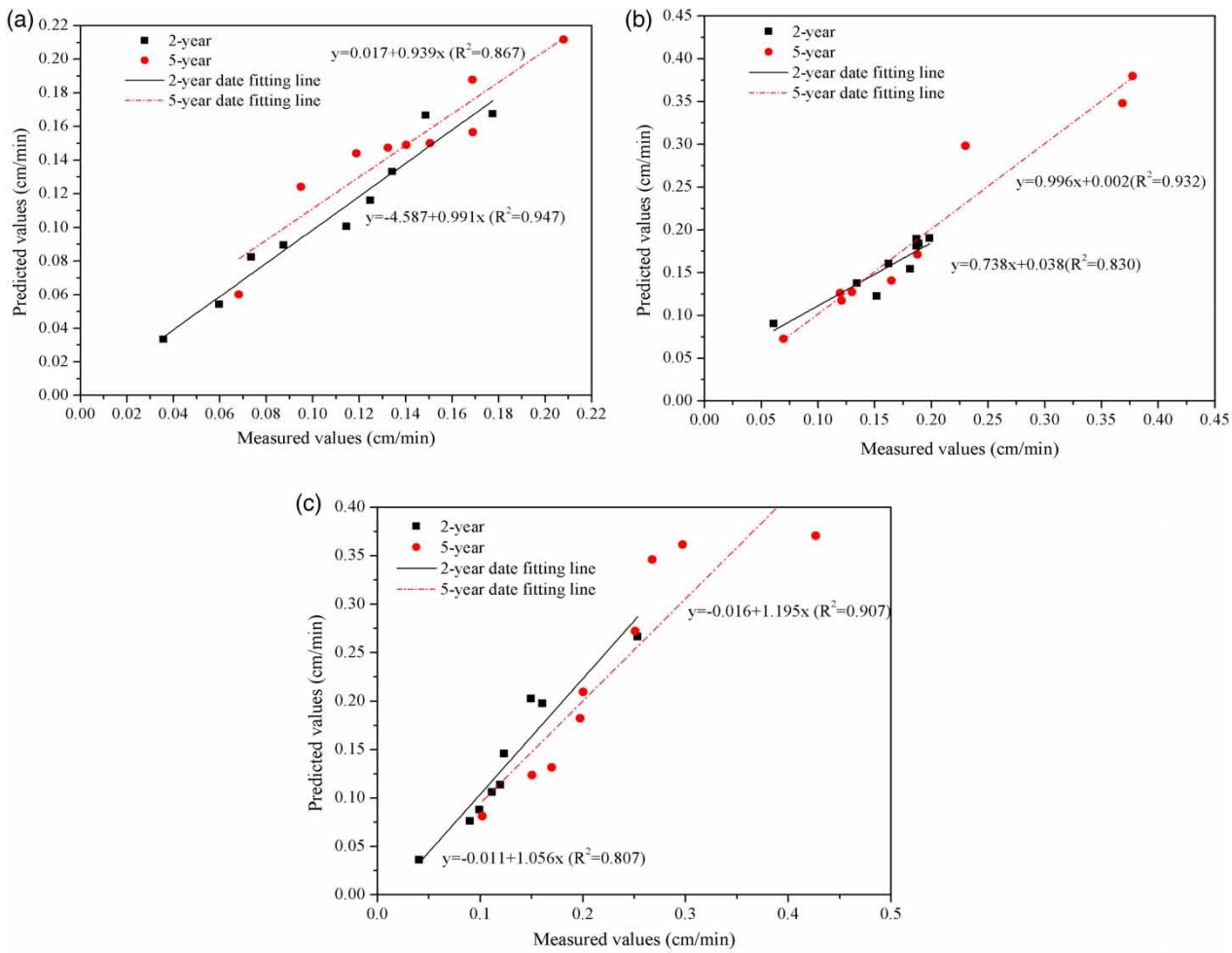

Figure 5 | Comparison of predicted and measured values: (a) tank #1, (b) tank #3, and (c) tank #4.

The error between the experimental value and the simulation value was caused by inflow and infiltration characteristics. A part preferential flow was caused by non-uniform inflow distribution and side wall flow. Evidently, the outflow of the bottom perforated tube would fluctuate and change. The current state of knowledge is inadequate for quantifying preferential flow. Simple mathematical tools for comparing data obtained with different approaches or different initial conditions would provide new information on a large number of studies, and better instrumentation is required for studying flow inside macropores and at the macropore–matrix interface, etc. Djabelkhir *et al.* (2017) developed a dual permeability approach in a hydrological modeling framework. Infiltration in macropores, which are connected to the surface, is activated when the first matrix layer reaches saturation. The results showed an underestimation of the flux infiltrated in the matrix surface and important infiltration in macropores with the new model, for most soil types, compared to Hydrus-1D. The difference between porosity and IR was significant in three tanks. A lower IR was correlated with a higher peak flow reduction rate, however, there is a risk of overflow and logging risks.

CONCLUSIONS

Taking media types and combinations as the objects in this study, a pilot-scale bioretention experiment was carried out to identify the effects of different influencing factors (IV, ADT, SZH, IR) on rainfall regulation. (i) Fly ash mixing sand (1:1, by volume) showed relatively steady water volume and peak flow reduction rates (58.6–67.9% and 72.0–86.4%), which was recommended for reducing rainfall runoff. The water volume reduction effect of tank #2 (BFSS, 1:1 by volume) was the highest in July under five-year design rainfall intensity and gradually declined with decreasing temperature. (ii) The relation model could be used to evaluate the water volume reduction effect of bioretention systems with different operating conditions, and water volume reduction rate and ADT or SZH were positively correlated, however, water volume reduction rate and IV or MI were negatively correlated. (iii) During the simulation of the water infiltration process using HYDRUS-1D, the predicted values were close to the measured values for #1, #3, and #4 systems. Tank #1 was relatively optimal. In future studies, field tests and a longer running simulation should be studied to better understand the water quality performance of bioretention systems.

ACKNOWLEDGEMENTS

This research was financially supported by the Key Research and Development Project of Shaanxi Province (2017ZDXM-SF-073) and National Natural Science Foundation of China (51879215).

REFERENCES

Baek, S. S., Ligaray, M., Park, J. P., Shin, H. S., Kwon, Y., Brascher, J. T. & Cho, K. H. 2017 Developing a hydrological simulation tool to design bioretention in a watershed. *Environ. Modell. Softw.* **11**, 1–12.

Brown, R. A., Skaggs, R. W. & Hunt, W. F. 2013 Calibration and validation of DRAINMOD to model bioretention hydrology. *J. Hydrol.* **486**, 430–442.

Cen, G. P., Shen, J. & Fan, R. 1998 Research on rainfall pattern of urban design storm. *Adv. Water Sci.* **9**, 41–46 (in Chinese).

Che, W. & Li, J. Q. 2006 *Urban Rainwater Utilization Technology and Management*. China Architecture & Building Press, Beijing, China (in Chinese).

Cipolla, S. S., Maglionico, M. & Stojkov, I. A. 2016 Long-term hydrological modelling of an extensive green roof by means of SWMM. *Ecol. Eng.* **95**, 876–887.

Davis, A. P., Traver, R. G., Hunt, W. F., Lee, R., Brown, R. A. & Olszewski, J. M. 2012 Hydrologic performance of bioretention storm-water control measures. *J. Hydrol. Eng.* **17**, 604–614.

Demuzere, M., Orru, K., Heidrich, O., Olazabal, E., Geneletti, D., Orru, H., Bhave, A. G., Mittal, N., Feliu, E. & Faehnle, E. 2014 Mitigating and adapting to climate change: multi-functional and multi-scale assessment of green urban infrastructure. *J. Environ. Manage.* **146**, 107–115.

Djabelkhir, K., Lauvernet, C., Kraft, P. & Carluer, N. 2017 Development of a dual permeability model within a hydrological catchment modeling framework: 1D application. *Sci. Total Environ.* **575**, 1429–1437.

Gülbaz, S. & Kazezyılmaz-Alhan, C. M. 2016 Experimental investigation on hydrologic performance of LID with rainfall-watershed-bioretention system. *J. Hydrol. Eng.* **22**, 1–10.

Hatt, B. E., Fletcher, T. D. & Deletic, A. 2009 Hydrologic and pollutant removal performance of storm water biofiltration systems at the field scale. *J. Hydrol.* **365**, 310–321.

Lee, J. Y., Moon, H. J., Kim, T. I., Kim, H. W. & Han, M. Y. 2013 Quantitative analysis on the urban flood mitigation effect by the extensive green roof system. *Environ. Pollut.* **181**, 257–261.

Liu, Y., Engel, B. A., Flanagan, D. C., Gitau, M. W., McMillan, S. K. & Chaubey, I. 2017 A review on effectiveness of best management practices in improving hydrology and water quality: needs and opportunities. *Sci. Total Environ.* **601–602**, 580–593.

Lu, J. S., Chen, Y., Zheng, Q., Du, R., Wang, S. P. & Wang, J. P. 2010 Derivation of rainstorm intensity formula in Xi'an City. *China Water Wastewater* **26**, 82–84 (in Chinese).

Mangangka, I. R., Liu, A., Egodawatta, P. & Goonetilleke, A. 2015 Performance characterization of a stormwater treatment bioretention basin. *J. Environ. Manage.* **150**, 173–178.

Nie, F. H. 2018 *Feasibility Study of Urban Landscape Green Space Reduce Surface Runoff and Pollution Load in Shanghai*. Tongji University, Shanghai, China (in Chinese).

Page, J. L., Winston, R. J., Mayes, D. B., Perrin, C. & Hunt, W. F. 2012 Retro fitting with innovative stormwater control measures: hydrologic mitigation of impervious cover in the municipal right-of-way. *J. Hydrol.* **527**, 923–932.

Payne, E. G. I., Fletcher, T. D., Cook, P. L. M., Deletic, A. & Hatt, B. E. 2014 Processes and drivers of nitrogen removal in stormwater biofiltration. *Crit. Rev. Env. Sci. Technol.* **44**, 796–846.

Ramos, T. B., Šimůnek, J., Gonçalves, M. C., Martins, J. C., Prazeres, A., Castanheira, N. L. & Pereira, L. S. 2011 Field evaluation of a multicomponent solute transport model in soils irrigated with saline waters. *J. Hydrol.* **407**, 129–144.

Sun, Y. W. & Wei, X. M. 2011 Global analysis of sensitivity of bioretention cell design elements to hydrologic performance. *Water Sci. Eng.* **4**, 246–257.

Versini, P. A., Kotelnikova, N., Poulhes, A., Tchiguirinskaia, I., Schertzer, D. & Leurent, F. 2018 A distributed modelling approach to assess the use of blue and green infrastructures to fulfil stormwater management requirements. *Landsc. Urban Plan.* **173**, 60–63.

Wang, Z. T., Jiao, X. X., Han, H. L. & Yu, X. B. 2013 Sensitivity analysis of VG model parameters with vertical one-dimensional soil infiltration. *J. Hohai Univ. (Natural Sciences)* **41**, 80–84.

Winston, R. J., Dorsey, J. D. & Hunt, W. F. 2016 Quantifying volume reduction and peak flow mitigation for three bioretention cells in clay soils in northeast Ohio. *Sci. Total Environ.* **553**, 83–95.

Yi, C. & Fan, J. 2016 Application of HYDRUS-1D model to provide antecedent soil water contents for analysis of runoff and soil erosion from a slope on the Loess Plateau. *Catena* **139**, 1–8.

Yin, R. X., Meng, Y. Y., Zhang, S. H. & Chen, J. G. 2015 Study on runoff of bioretention by model simulation. *J. China Hydrol.* **35**, 28–35 (in Chinese).

First received 16 February 2019; accepted in revised form 17 May 2019. Available online 7 June 2019